This is a repository copy of *Effect of gas properties on the dynamics of the electrical slope asymmetry effect in capacitive plasmas:comparison of Ar, H2 and CF4*.

White Rose Research Online URL for this paper:
https://eprints.whiterose.ac.uk/101173/

Version: Published Version

Article:

Letter

Effect of gas properties on the dynamics of the electrical slope asymmetry effect in capacitive plasmas: comparison of Ar, H$_2$ and CF$_4$

B Bruneau[1], T Lafleur[2], T Gans[3], D O'Connell[3], A Greb[3], I Korolov[4], A Derzsi[4], Z Donkó[4], S Brandt[5], E Schüngel[5], J Schulze[5], P Diomede[6,7], D J Economou[6], S Longo[8], E Johnson[1] and J-P Booth[2]

[1] LPICM-CNRS, Ecole Polytechnique, 91128 Palaiseau, France
[2] LPP, Ecole Polytechnique-CNRS-Uni Paris-Sud-UPMC, 91128 Palaiseau, France
[3] York Plasma Institute, Department of Physics, University of York, Heslington, York, YO10 5DD, UK
[4] Institute for Solid State Physics and Optics, Wigner Research Centre for Physics, Hungarian Academy of Sciences, Konkoly-Thege Miklós str. 29-33, H-1121 Budapest, Hungary
[5] Department of Physics, West Virginia University, Morgantown, West Virginia 26506-6315, USA
[6] Plasma Processing Laboratory, Department of Chemical & Biomolecular Engineering, University of Houston, Houston, TX 77204-4004, USA
[7] FOM Institute DIFFER—Dutch Institute for Fundamental Energy Research, P. O. Box 6336, 5600 H H Eindhoven, The Netherlands
[8] Dipartimento di Chimica, Universita' degli studi di Bari, via Orabora 4, 70126 Bari, Italy

E-mail: bastien.bruneau@polytechnique.edu

CrossMark

Abstract

Tailored voltage excitation waveforms provide an efficient control of the ion energy (through the electrical asymmetry effect) in capacitive plasmas by varying the 'amplitude' asymmetry of the waveform. In this work, the effect of a 'slope' asymmetry of the waveform is investigated by using sawtooth-like waveforms, through which the sheath dynamic can be manipulated. A remarkably different discharge dynamic is found for Ar, H$_2$, and CF$_4$ gases, which is explained by the different dominant electron heating mechanisms and plasma chemistries. In comparison to Argon we find that the electrical asymmetry can even be reversed by using an electronegative gas such as CF$_4$. Phase resolved optical emission spectroscopy measurements, probing the spatiotemporal distribution of the excitation rate show excellent agreement with the results of particle-in-cell simulations, confirming the high degree of correlation between the excitation rates with the dominant heating mechanisms in the various gases. It is shown that, depending on the gas used, sawtooth-like voltage waveforms may cause a strong asymmetry.

Keywords: tailored voltage waveforms, electrical asymmetry effect, sawtooth waveforms, electron heating, PIC modeling, PROES

(Some figures may appear in colour only in the online journal)

Going beyond classic dual-frequency capacitive plasmas between two parallel electrodes [1–6], discharges excited by tailored voltage waveforms (TVWs), comprising a fundamental signal frequency in the radio frequency (RF) domain combined with higher harmonics with controlled phases and amplitudes, have been investigated in recent years [7–15]. Amplitude asymmetry of the waveform, i.e. the difference between its maximum and its minimum value, and the associated dynamics occurring in these plasmas have previously been studied for the separate control of ion energy and flux due to the electrical asymmetry effect (EAE) [16–19].

Recently, a new type of temporally asymmetric TVW was proposed, called 'sawtooth' waveforms [20–22], comprising a fast rise and a slow fall, or vice versa. These waveforms present a slope asymmetry but no amplitude asymmetry. In argon this was shown to induce different sheath motions in front of the two electrodes, leading to strong ionization close to the electrode where the sheath expansion is fast, with only weak ionization close to the electrode where the sheath expansion is slow [22]. However, in molecular, electronegative plasmas significantly different physics phenomena can occur. For example, ionization mechanisms, other than sheath expansion, have been observed [23–25]. This letter compares sawtooth-excited discharges operated in gases with distinctly different properties, namely argon (Ar, electropositive), hydrogen (H_2, light molecular gas), and carbon tetrafluoride (CF_4, electronegative). For each gas, experimental data are compared to specific particle-in-cell (PIC) simulations. For Ar we used the code developed by Lafleur [26], for H_2 that of the Bari University group [27, 28], and for CF_4 the code from the Wigner Research Centre for Physics [18].

The experimental setup is displayed in figure 1. A reactor comprising 20 cm diameter parallel electrodes with an inter-electrode gap of 2.5 cm was made geometrically symmetric by adding a thick Teflon ring (inner diameter 10 cm), fitted with a $2.5 \times 2.5 \times 10$ cm borosilicate glass window to allow optical access. The voltage waveform is generated as presented in detail in [8], without any impedance matching. An impedance-matched generator has been proposed by Franek *et al* [29], but was not employed here as a high coupled power was not required. After an iterative waveform optimization (using the method of Patterson *et al* [30]) the desired waveform (shown in blue for a sawtooth with $n = 5$ frequencies) can be generated at the powered electrode. The gate of the intensified CCD camera (Andor iStar) used for phase resolved optical emission spectroscopy (PROES) measurements is synchronized to the RF generation system via a delay generator. A 2 ns gate was used, providing 91 images within one RF-cycle for a fundamental frequency of 5.5 MHz. The respective emission lines (750.4 nm for Ar, 656 nm (H-alpha) for H_2, and 703.7 nm (F atom) for CF_4,) were selected using interference filters. In all cases, the electron impact excitation rate was deduced from the measured emission by deconvoluting the radiative lifetime of the emitting state [31].

Since in any experiment the voltage waveforms delivered have a finite frequency bandwidth, the voltage waveforms used are approximations of an ideal sawtooth, where a waveform consisting of a slow decrease and an infinitely fast increase is referred to as a 'sawtooth-down'. The approximation is performed by truncating the Fourier series for a perfect sawtooth

waveform after n harmonics according to equation (1) (with a positive sign for sawtooth-down),

$$V_{ac}(t) = \pm V_0 \sum_{k=1}^{n} \frac{1}{k} \sin(k\omega t), \qquad (1)$$

where V_{ac} is the voltage applied to the powered electrode, ω is the fundamental angular frequency, and V_0 is adjusted to give the desired peak-to-peak voltage V_{PP}. Alternatively, 'sawtooth-up' waveforms (equation (1), minus sign) can be used. In a geometrically symmetric reactor this signal inversion produces a reversal of the roles of each electrode. The experiments were carried out at pressures of 400 mTorr, 900 mTorr, and 600 mTorr, for Ar, H_2, and CF_4, respectively. The exact value of the pressure has a negligible effect on the qualitative features shown hereafter. For example, it was shown in [21] that only a 5% increase of the ion flux ratio was obtained by increasing the pressure from 400 mTorr to 800 mTorr in Ar. The peak-to-peak voltage V_{PP} was set to 250 V, 350 V, and 400 V for Ar, H_2, and CF_4 respectively.

Figure 2 compares the experimental results and simulations for the three gases using a sawtooth-down waveform with $n = 5$ (corresponding to the waveform displayed in figure 1). The results for Ar, H_2, and CF_4 are displayed from top to bottom. The x-axis represents position (with the powered electrode at $x = 0$ cm and the grounded electrode at $x = 2.5$ cm), while the y-axis represents time, and spans one fundamental RF cycle. The first column shows the excitation rate, K_{exc}, of the respective observed emitting states, as derived from PROES measurements. The next three columns display simulation results. The second column shows the excitation rate, K_{exc}, while the third shows the electric field distribution, $E(x, t)$ divided by V_{PP}, outside of the sheath regions (which are shown in black). The same scale is used for the three gases, so that the normalized electric field values can be directly compared. The fourth column shows the electron power absorption, S_e. The sheath edge position was determined using Brinkmann's criterion [32], and the sheath edge position is shown as a white line in the second and fourth columns. For all three gases the simulations show fast sheath expansion and slow sheath contraction in front of the grounded electrode, and slow sheath expansion with fast sheath contraction in front of the powered electrode, as expected from the sawtooth-down waveform used.

Looking at the excitation rate, one can see that an excellent agreement is found between experiments and simulations for all three gas chemistries, despite significantly different excitation features between them. In Ar, excitation is strongly localized close to the grounded electrode, and occurs during the fast sheath expansion (as indicated by the simulations in the second column). Only very weak excitation is observed close to the powered electrode during the (much slower) sheath expansion. In contrast, for H_2 two excitation peaks of similar amplitude occur almost simultaneously, the first one close to the grounded electrode where the sheath is expanding rapidly (sheath expansion heating) and a second peak close to the powered electrode where the sheath is contracting rapidly (due to a reversed electric field). Finally, in CF_4, weak excitation occurs close to the grounded electrode during the
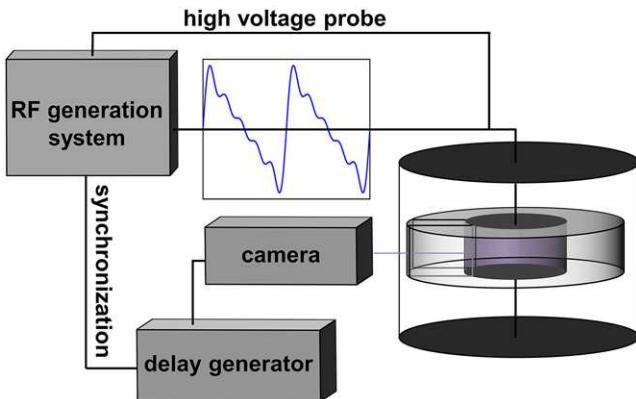
Figure 1. Schematic of the experimental setup with RF generation system, delay generator and ultrafast camera for PROES measurements.

fast expansion, followed by a strong peak very close to the powered electrode during the fast sheath contraction. In order to understand the difference in the excitation features between the gas chemistries, both the electric field and the electron power absorption were analyzed.

In Ar, no significant electric field is observed within the bulk plasma outside of the sheath regions (the green color indicates zero field). In contrast, in H_2, a strong positive electric field occurs close to the powered electrode during the fast sheath contraction, corresponding to an electric field reversal. It should be noted that, although smaller, a field reversal also occurs at the grounded electrode when the sheath collapses. These field reversals occur because the motion of electrons is hindered by collisions (which are much more significant in H_2, a molecular gas, compared to Ar), and therefore a significant (reversed) electric field is necessary to accelerate the electrons to the electrodes and balance the escaping ion current [33]. The intensity of these field reversals therefore only depends on how fast the sheath contracts. When the sheath at the powered electrode is contracting rapidly the electron thermal flux is too low to ensure current balance, and a high, reversed, electric field is necessary. In contrast, the sheath contraction at the grounded electrode is slow, and therefore a weaker reversed electric field is sufficient to ensure current balance.

In CF_4, a very strong electric field (much stronger than in H_2) is observed during the fast sheath contraction. This electric field builds up because of the low electron density (because the majority of electrons have been converted to heavy F^- ions by dissociative attachment to CF_4), leading to low conductivity. In this discharge, the negative ion density (not shown), is particularly high close to the electrode where fast sheath contraction occurs (in this case the powered electrode), hence the electron density and the conductivity are particularly low. In contrast, close to the opposite (grounded) electrode the negative ion density is significantly lower and the electron density is higher, and therefore the conductivity is higher. As a consequence, a strong electric field is only observed close to the powered electrode, where fast sheath contraction occurs. Furthermore, on approaching the powered electrode, this positive electric field (corresponding to field reversal) is followed by a negative electric field, therefore creating an electric

potential well, which acts as a trap for the electrons at one moment in time and limits their flux to the electrode.

The electron power absorption dynamics (shown in the fourth column) is clearly strongly affected by the gas properties. In all cases (for these relatively high gas pressure plasmas) the maximum in the electron power absorption occurs close to where the highest excitation rate is observed. This is because the electron mean free path is short compared to the discharge length. In Ar strong electron power absorption occurs close to the grounded electrode during the fast sheath expansion, while much lower electron power absorption occurs near the powered electrode during the slow sheath expansion. This is consistent with the hard wall model of Godyak [34, 35], according to which, the faster the sheath expansion rate, the greater the electron energy gain. In addition, because there is no significant electric field in the plasma bulk, and because secondary electron emission from the electrodes plays no significant role under these conditions, there is no other source of energy gain for the electrons. The discharge therefore operates in α-mode. In H_2, the situation is more complex: strong electron power absorption again occurs close to the grounded electrode during the fast sheath expansion, but is immediately followed by a second electron power absorption peak of similar amplitude, close to the powered electrode, due to the electric field reversal in this region. These two power absorption peaks are therefore the cause for the two excitation peaks.

In CF_4, the situation is again different. While some weak electron power absorption can be observed close to the grounded electrode during the fast sheath expansion, the largest power absorption peak is observed close to the powered electrode during the fast sheath contraction. Indeed, the large reversed electric field during this period strongly accelerates electrons from the plasma bulk towards the powered electrode. This leads to significant power absorption, accelerating electrons up to a mean energy of about 10 eV at this point. Because the electric fields in this phase can be split into drift and ambipolar components, this heating mode has been named the 'drift-ambipolar' (DA) mode [24]. This power absorption peak again coincides with a strong excitation peak. The latter is further strengthened by the formation of a potential well, which traps the energetic electrons and reduces their loss to the electrode, hence increasing the probability for these electrons to excite the neutral gas. In addition, this electron confinement increases the probability of electron attachment, and therefore the generation of negative ions. This further decreases the conductivity, and therefore increases the reversed electric field, forming a positive feedback loop.

In short, sawtooth waveforms induce a strong asymmetry in the excitation rate in both the Ar and CF_4 cases. However, the location of maximal excitation in CF_4 is opposite that of Ar, due to the change in the dominant electron power absorption mechanism. In the case of H_2, any asymmetry is cancelled out as both mechanisms occur almost simultaneously.

From the location of the electron excitation (figure 2, first and second columns) one would expect differences in the ion fluxes to the grounded and powered electrodes. Figure 3(a) shows the ratio β, of the ion flux to the powered electrode divided by that to the grounded electrode, for Ar (black
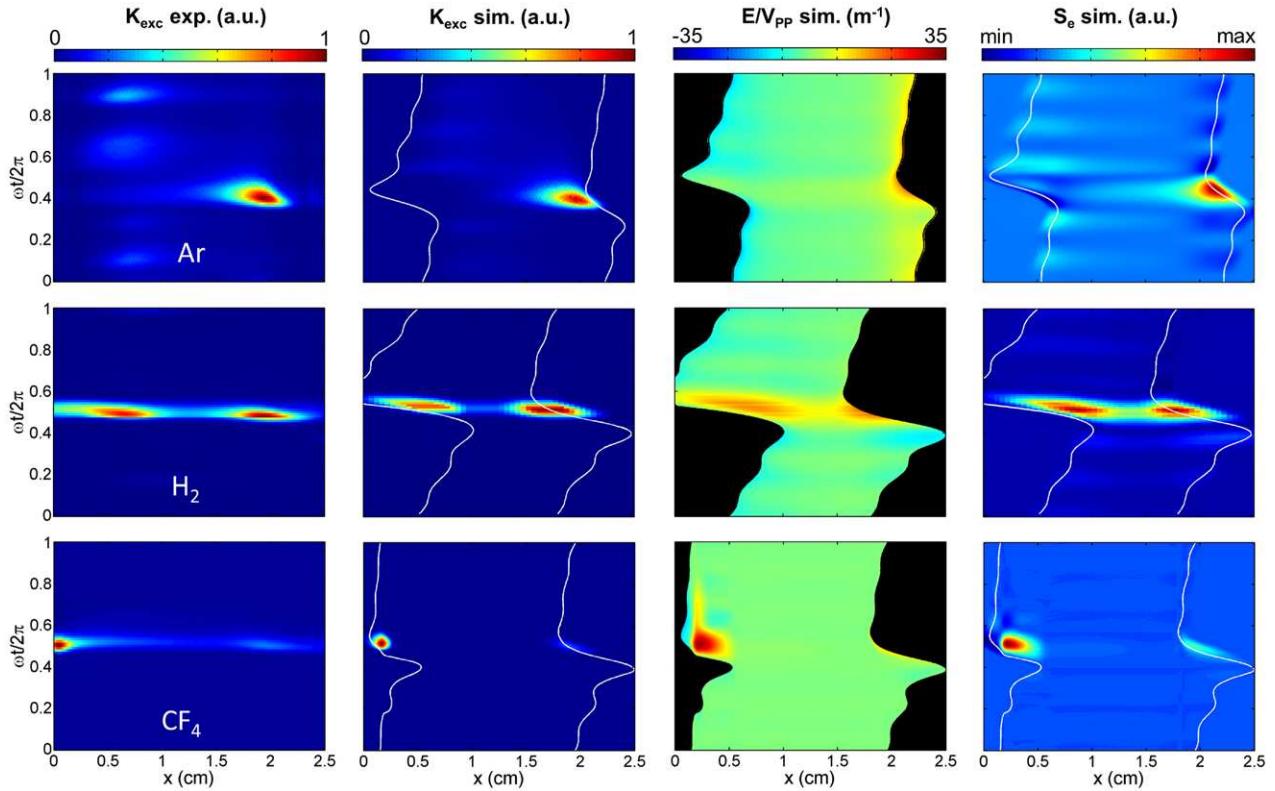
Figure 2. Excitation rate obtained from the experiments (first column), and from the simulations (second column), spatiotemporal plots of the electric field (third column), and electron power absorption rate (fourth column), from the simulations, for an argon discharge (top row), a hydrogen discharge (middle row), and a carbon tetrafluoride discharge (bottom row).
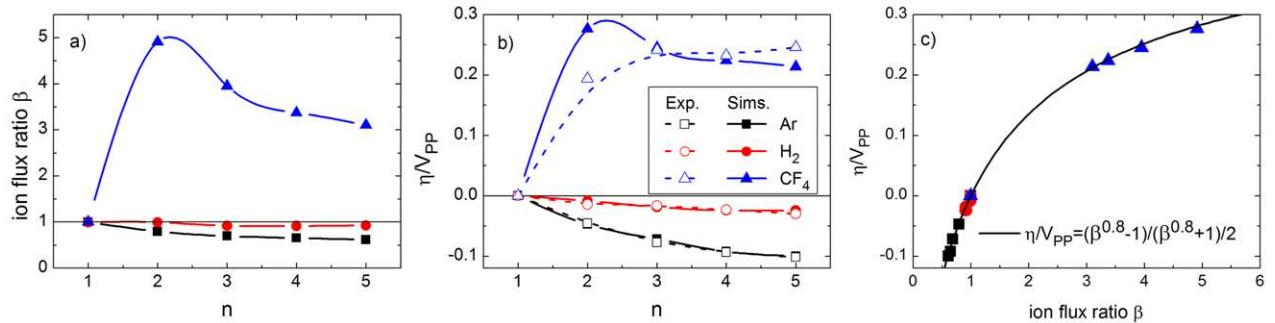
Figure 3. (a) Ion flux ratio β obtained by simulations for Ar (black squares), H_2 (red circles), and CF_4 (blue triangles) discharges, (b) normalized dc self-bias voltage, from simulations (full symbols) and from experiments (empty symbols), obtained with sawtooth-like waveforms composed of n frequencies. (c) Normalized dc self-bias voltage as a function of the ion flux ratio for the three gases.

squares), H_2 (red circles), and CF_4 (blue triangles) discharges, obtained from simulations, as a function of the number of applied harmonics n. This ratio exceeds unity for CF_4, because the (phase-integrated) excitation and ionization maxima are localized close to the powered electrode. In contrast, the ratio is below one for Ar, because the majority of the excitation and ionization occurs near the grounded electrode. It is worth noting that the asymmetry in the ion flux obtained for CF_4 is not only opposite compared to Ar, it is also significantly larger. As one can see, an ion flux ratio of about five can be obtained in a geometrically symmetric reactor with CF_4, while this drops to 0.6 (corresponding to an ion flux 1.6 times larger

at the grounded electrode) in the case of Ar under these conditions. Finally, for H_2 the ion flux ratio remains close to unity (it is always between 0.9 and 1), since no clear asymmetry is observed in the spatial profile of the excitation dynamics.

In capacitively coupled plasmas, a dc self-bias voltage establishes such as to equalize the period-averaged electron and ion fluxes to the electrodes. Figure 3(b) shows the dc self-bias voltage, η, normalized to the peak-to-peak voltage V_{PP}, obtained from simulations (full symbols), and experiments (empty symbols), showing excellent agreement (with the exception of $n = 2$ in CF_4, for reasons not yet known). In CF_4, η is always positive, whereas it is always negative in Ar and

H_2. It is worth noting that a strong correlation exists between the ion flux ratio, β, and η. The sign of η will be positive if $\beta > 1$, and negative if $\beta < 1$. Its amplitude is proportional to the difference of β from unity. This link can be understood by considering the expression for η given by Heil *et al* [1] applied to the case of sawtooth waveforms (which have no amplitude asymmetry):

$$\eta = -\frac{V_{PP}}{2} \times \frac{1 - \varepsilon}{1 + \varepsilon} \qquad (2)$$

where ε is the symmetry parameter, which can be approximated by the ratio of the mean ion densities in the sheath at the powered and grounded electrode. Because the mean ion densities and the ion fluxes are strongly linked, we can expect a relationship between ε and β. Assuming a power law, $\varepsilon = \beta^a$ (because we should have $\varepsilon = 1$ when $\beta = 1$, and $\varepsilon \to 1/\varepsilon$ when $\beta \to 1/\beta$), where a is a fitting parameter, and replacing ε by its expression as a function of β in equation (2), it is possible to obtain a relationship between the normalized dc self-bias voltage and the ion flux ratio. Figure 3(c) shows η/V_{PP} as a function of β, for the three gases and for different values of n. Also shown in black is the best fit obtained by replacing ε by its expression as a function of β in equation (2). We find $a = 0.8$, indicating that the ion flux ratio is always larger than the symmetry parameter. The agreement is excellent for all three gases and for all conditions, suggesting that this relationship may have general applicability.

In conclusion, we have observed that the charged particle dynamics occurring in plasmas of gases with different properties leads to fundamental differences in the spatial asymmetry of discharges excited with the same sawtooth waveform. The spatiotemporal distribution of the dominant electron energy gain mechanism is identified as the main cause for these asymmetries. When the discharge is in α-mode (Ar), most of the ionization occurs close to the electrode where the fast sheath expansion occurs, whereas in a strongly electro-negative gas where the DA mode dominates (CF_4) ionization is predominantly close to the electrode where fast sheath contraction occurs. Hydrogen discharges were found to operate in a mixed mode, where significant ionization is simultaneously observed near both sheath edges when they contract or expand quickly. The net effect for such H_2 discharges is an absence of asymmetry in the spatial profile of the time-averaged ionization. Finally, despite these differences, a power-law relationship is observed between the ion flux ratio and the normalized dc self-bias, and a single value of exponent fits the data for all three gas chemistries studied herein.

Acknowledgments

References

[1] Goto H H, Löwe H-D and Ohmi T 1992 Dual excitation reactive ion etcher for low energy plasma processing *J. Vac. Sci. Technol.* A **10** 3048–54

[2] Kitajima T, Takeo Y, Petrović Z L and Makabe T 2000 Functional separation of biasing and sustaining voltages in two-frequency capacitively coupled plasma *Appl. Phys. Lett.* **77** 489–91

[3] Boyle P C, Ellingboe A R and Turner M M 2004 Independent control of ion current and ion impact energy onto electrodes in dual frequency plasma devices *J. Phys. Appl. Phys.* **37** 697

[4] Georgieva V, Bogaerts A and Gijbels R 2004 Numerical investigation of ion-energy-distribution functions in single and dual frequency capacitively coupled plasma reactors *Phys. Rev.* E **69** 026406

[5] Turner M M and Chabert P 2006 Collisionless heating in capacitive discharges enhanced by dual-frequency excitation *Phys. Rev. Lett.* **96** 205001

[6] Chabert P and Braithwaite N 2011 *Physics of Radio-Frequency Plasmas* (Cambridge: Cambridge University Press) [Online] available: www.cambridge.org/us/academic/subjects/physics/plasma-physics-and-fusion-physics/physics-radio-frequency-plasmas [Accessed: 3 April 2015]

[7] Heil B G, Czarnetzki U, Brinkmann R P and Mussenbrock T 2008 On the possibility of making a geometrically symmetric RF-CCP discharge electrically asymmetric *J. Phys. Appl. Phys.* **41** 165202

[8] Johnson E V, Verbeke T, Vanel J-C and Booth J-P 2010 Nanocrystalline silicon film growth morphology control through RF waveform tailoring *J. Phys. Appl. Phys.* **43** 412001

[9] Lafleur T, Boswell R W and Booth J P 2012 Enhanced sheath heating in capacitively coupled discharges due to non-sinusoidal voltage waveforms *Appl. Phys. Lett.* **100** 194101

[10] Lafleur T, Delattre P A, Johnson E V and Booth J P 2012 Separate control of the ion flux and ion energy in capacitively coupled radio-frequency discharges using voltage waveform tailoring *Appl. Phys. Lett.* **101** 124104

[11] Coumou D J, Clark D H, Kummerer T, Hopkins M, Sullivan D and Shannon S 2014 Ion energy distribution skew control using phase-locked harmonic RF bias drive *IEEE Trans. Plasma Sci.* **42** 1880–93

[12] Zhang Q-Z, Zhao S-X, Jiang W and Wang Y-N 2012 Separate control between geometrical and electrical asymmetry effects in capacitively coupled plasmas *J. Phys. Appl. Phys.* **45** 305203

[13] Zhang Y, Zafar A, Coumou D J, Shannon S C and Kushner M J 2015 Control of ion energy distributions using phase shifting in multi-frequency capacitively coupled plasmas *J. Appl. Phys.* **117** 233302

[14] Gibson A R, Greb A, Graham W G and Gans T 2015 Tailoring the nonlinear frequency coupling between odd harmonics for the optimisation of charged particle dynamics in capacitively coupled oxygen plasmas *Appl. Phys. Lett.* **106** 054102

[15] Schüngel E, Mohr S, Schulze J, Czarnetzki U and Kushner M J 2014 Ion distribution functions at the

electrodes of capacitively coupled high-pressure hydrogen discharges *Plasma Sources Sci. Technol.* **23** 015001

[16] Donkó Z, Schulze J, Czarnetzki U, Derzsi A, Hartmann P, Korolov I and Schüngel E 2012 Fundamental investigations of capacitive radio frequency plasmas: simulations and experiments *Plasma Phys. Control. Fusion* **54** 124003

[17] Schüngel E, Brandt S, Donkó Z, Korolov I, Derzsi A and Schulze J 2015 Electron heating via self-excited plasma series resonance in geometrically symmetric multi-frequency capacitive plasmas *Plasma Sources Sci. Technol.* **24** 044009

[18] Schulze J, Derzsi A and Donkó Z 2011 Electron heating and the electrical asymmetry effect in dual-frequency capacitive CF$_4$ discharges *Plasma Sources Sci. Technol.* **20** 045008

[19] Derzsi A, Korolov I, Schüngel E, Donkó Z and Schulze J 2013 Electron heating and control of ion properties in capacitive discharges driven by customized voltage waveforms *Plasma Sources Sci. Technol.* **22** 065009

[20] Bruneau B, Novikova T, Lafleur T, Booth J P and Johnson E V 2014 Ion flux asymmetry in radiofrequency capacitively-coupled plasmas excited by sawtooth-like waveforms *Plasma Sources Sci. Technol.* **23** 065010

[21] Bruneau B, Novikova T, Lafleur T, Booth J P and Johnson E V 2015 Control and optimization of the slope asymmetry effect in tailored voltage waveforms for capacitively coupled plasmas *Plasma Sources Sci. Technol.* **24** 015021

[22] Bruneau B, Gans T, O'Connell D, Greb A, Johnson E V and Booth J-P 2015 Strong ionization asymmetry in a geometrically symmetric radio frequency capacitively coupled plasma induced by sawtooth voltage waveforms *Phys. Rev. Lett.* **114** 125002

[23] Greb A, Niemi K, O'Connell D and Gans T 2013 The influence of surface properties on the plasma dynamics in radio-frequency drivenoxygen plasmas: measurements and simulations *Appl. Phys. Lett.* **103** 244101

[24] Schulze J, Derzsi A, Dittmann K, Hemke T, Meichsner J and Donkó Z 2011 Ionization by drift and ambipolar electric fields in electronegative capacitive radio frequency plasmas *Phys. Rev. Lett.* **107** 275001

[25] Dittmann K, Küllig C and Meichsner J 2012 Electron and negative ion dynamics in electronegative cc-rf plasmas *Plasma Phys. Control. Fusion* **54** 124038

[26] Lafleur T and Booth J P 2012 Control of the ion flux and ion energy in CCP discharges using non-sinusoidal voltage waveforms *J. Phys. Appl. Phys.* **45** 395203

[27] Diomede P, Longo S, Economou D J and Capitelli M 2012 Hybrid simulation of a dc-enhanced radio-frequency capacitive discharge in hydrogen *J. Phys. Appl. Phys.* **45** 175204

[28] Diomede P, Economou D J, Lafleur T, Booth J-P and Longo S 2014 Radio-frequency capacitively coupled plasmas in hydrogen excited by tailored voltage waveforms: comparison of simulations with experiments *Plasma Sources Sci. Technol.* **23** 065049

[29] Franek J, Brandt S, Berger B, Liese M, Barthel M, Schüngel E and Schulze J 2015 Power supply and impedance matching to drive technological radio-frequency plasmas with customized voltage waveforms *Rev. Sci. Instrum.* **86** 053504

[30] Patterson M M, Chu H-Y and Wendt A E 2007 Arbitrary substrate voltage wave forms for manipulating energy distribution of bombarding ions during plasma processing *Plasma Sources Sci. Technol.* **16** 257–64

[31] Gans T, O'Connell D, der Gathen V S and Waskoenig J 2010 The challenge of revealing and tailoring the dynamics of radio-frequency plasmas *Plasma Sources Sci. Technol.* **19** 034010

[32] Brinkmann R P 2007 Beyond the step model: approximate expressions for the field in the plasma boundary sheath *J. Appl. Phys.* **102** 093303

[33] Czarnetzki U, Luggenhölscher D and Döbele H F 1999 Space and time resolved electric field measurements in helium and hydrogen RF-discharges *Plasma Sources Sci. Technol.* **8** 230

[34] Godyak V A 1972 Statistical heating of electrons at an oscillating plasma boundary *Sov. Phys. - Tech. Phys.* **16** 1073

[35] Lieberman M A and Lichtenberg A J 2005 *Principles of Plasma Discharges and Materials Processing* (Hoboken, NJ: Wiley)